Research Inventy: International Journal of Engineering And Science
Vol.13, Issue 12 (December 2023), PP 74-84
Issn (e): 2278-4721, Issn (p):2319-6483, www.researchinventy.com

Comparative Study of Spectral Mismatch Factor, Color Parameters, and Uncertainty Evaluations for Different Outdoor Lamps.

Manal A. Haridy[1,*]
1 Photometry and Radiometry Division, National Institute of Standards (NIS), Giza, Egypt.
** Corresponding author: manal_haridi@yahoo.com*

Abstract
Spectral mismatch arises when the spectral distribution of light from artificial light sources differs from a photometer's sensitivity curve, impacting how the photometer perceives emitted light. Various lamp types emit light with distinct spectral distributions, influencing the photometer's ability to measure light intensity across wavelengths based on the human eye's sensitivity V (λ). This discrepancy causes inaccuracies as the photometer might not detect all lamp wavelengths, leading to spectral mismatch. Chromaticity color coordinates for lamps are essential descriptors of artificial light. Represented on a chromaticity diagram these coordinates depict a lamp's color emission based on its spectral distribution relative to the spectral locus. Different lamps yield distinct coordinates. These coordinates are pivotal in assessing color rendering accuracy, determining color temperature. They aid in selecting appropriate lighting for specific settings, maintaining desired color appearances, and ensuring uniform color output in diverse applications, serving as a foundational guide for both manufacturers and users. Evaluating any color measurement now involves considering the associated uncertainty. A set up based on NIS spectroradiometer, and the photometric bench used for measurements. This study involves determining spectral mismatch correction factor and chromaticity color coordinates across seven different outdoor lamps against NIS Secondary Standard Lamps from their spectral power distributions. Also evaluates the uncertainty due to spectral mismatch correction factors and chromaticity color coordinates. The results of spectral mismatch correction factors show that these mismatch values, chromaticity color coordinates values, and their uncertainties could be added to the of luminous flux and color measurements as corrections.

Keywords: *Uncertainty, Spectral mismatch correction factor, Spectral Power Distribution (SPD), Human response curve V (λ), chromaticity color coordinates, Uniform color space, Neon, Mercury, Mercury Vapor, Low Pressure Sodium, Ceramic Metal Halide, High Pressure Sodium, and Metal Halide Lamps.*

Date of Submission: 09-12-2023 Date of acceptance: 25-12-2023

I. Introduction

Outdoor lamps are crucial for safety, security, and aesthetics in outdoor spaces. They provide essential visibility at night, making streets and public areas safer to navigate while also deterring crime by illuminating dark areas. These lights extend the hours for outdoor activities and events, contributing to recreation and community gatherings. Moreover, they enhance the beauty and ambiance of outdoor environments, highlighting architectural elements and landscapes. In the field of photometry, the key instrument used is the photometer. Given that no photometer perfectly aligns with the V (λ) curve, it becomes crucial to gauge how closely we approximate this curve. Photometers produce a singular output value, aggregating data across the spectral range internally to yield this value. Typically, most photometers are calibrated using the CIE Illuminant A, a smooth spectral light source akin to a blackbody radiator functioning at 2856K. However, when these devices measure light sources with spectral distributions differing from the CIE Illuminant A, discrepancies arise due to spectral mismatch. To rectify this, a spectral mismatch correction factor is applied. This correction addresses the error emerging when a photometer measures a light source whose spectral power distribution doesn't align with the standard source used during the photometer's calibration. Correcting this spectral mismatch involves characterizing the photometer's relative spectral responsivity, leading to the derivation of the spectral mismatch factor (SMF). This factor becomes pivotal in rectifying errors stemming from spectral discrepancies between measured and standardized light sources [1]. Integrating spheres collect electromagnetic radiation from an external source to measure flux or optical attenuation. By reflecting radiation within their walls, they evenly spread it for straightforward detection by a sensor. These spheres are adaptable, able to measure sizable low-power beams, unaffected by alignment or coherence issues, and resilient against damage, particularly from short pulses. Their flexibility enables the use of diverse measurement methods. [2, 3]. The 1931 color matching

functions are fundamental to understanding human perception of color. Developed by the CIE, these functions represent how the human eye responds to different wavelengths of light through three primary colors: red, green, and blue. They define the spectral sensitivity of the eye by quantifying the amount of each primary color needed to match any given wavelength of light. This groundbreaking work laid the groundwork for modern color theory, enabling the creation of color spaces and models used across various industries. By establishing a standardized method for understanding how humans perceive color, the 1931 color matching functions revolutionized fields like imaging technology, color reproduction in visual arts, and the design of displays and lighting systems. The 1931 color matching functions remain highly influential despite subsequent refinements and advancements in color science. They are the cornerstone of colorimetry, providing a universal language for describing and reproducing colors accurately. These functions facilitated the development of color spaces like RGB (Red, Green, and Blue) and XYZ, forming the basis for color models used in digital imaging, television, computer graphics, and other visual technologies. Moreover, they continue to be a vital reference point in fields such as color calibration, where precise color reproduction is essential, ensuring consistency and fidelity in various applications where accurate color representation is paramount [4]. In 1976, the CIE introduced the Uniform Chromaticity Scale (UCS), a pivotal advancement in color science. The UCS aimed to improve the visual consistency of the xy-diagram, used for depicting color coordinates. While the original diagram, part of the CIE 1931 color spaces, was valuable, it had flaws in representing perceptual differences among colors, leading to inconsistencies in color display and perception. The UCS, implemented by the CIE in 1976, aimed to rectify these issues by enhancing the visual uniformity of the xy-diagram. By redefining color coordinates, it created a more consistent and perceptually accurate representation of colors. This refinement maintained the original system's useful features while significantly improving color science, aiding industries like printing, displays, and photography in managing and understanding colors more effectively. The adoption of the UCS by the CIE marked a crucial step toward achieving a more accurate and uniform portrayal of colors, benefiting various color-related technologies. In any field of measurement, precision demands a meticulous evaluation of uncertainties, as outlined in the ISO Guide to the Expression of Uncertainty in Measurement [5]. This guide serves as a cornerstone in national metrology institutes, ensuring that calibration laboratories receive measurements that can be traced back accurately. Assessing uncertainty in color measurements is particularly challenging yet crucial, as any color assessment lacks completeness without considering its accompanying uncertainty. To tackle this challenge, both the principles from the ISO Guide to the Expression of Uncertainty in Measurement [5] and J. L. Gardner's methods in color measurements [6,7] are employed. These methodologies are utilized to gauge uncertainties in chromaticity coordinates and uniform color spaces for select NIS luminous flux secondary and working standard lamps.

In this study, the spectral power distribution of the NIS secondary and working standard lamps measured which are crucial for assessing total luminous flux. These measurements entailed using the NIS setup, which consists of an optical bench and a spectroradiometer. The spectral mismatch factor, chromaticity color coordinates, and estimated uncertainty are calculated for all different outdoor lamps.

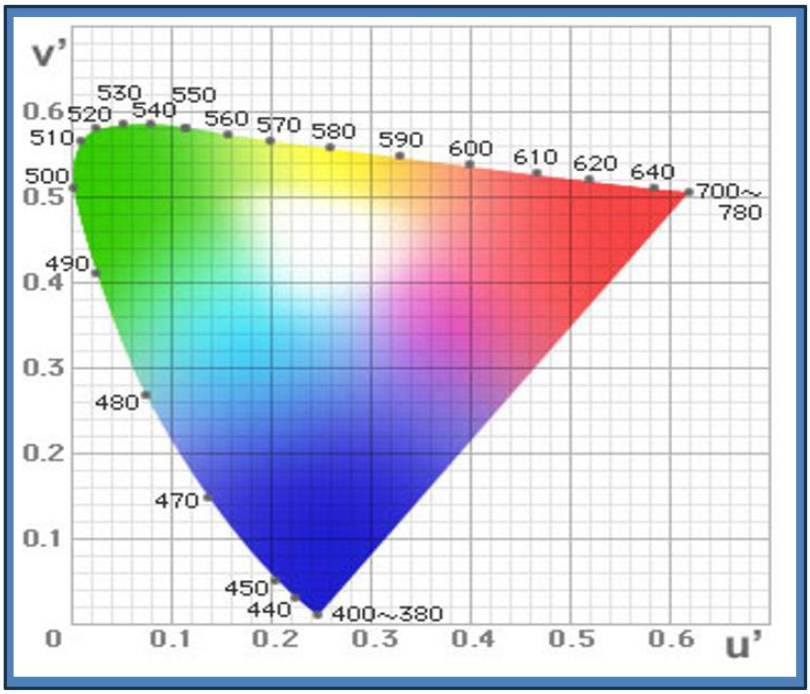

Figure-1. The 1976 CIE Chromaticity Diagram of Color Coordinates u' and v'.

II. Theoretical principles

2.1 Determination of Spectral Mismatch Factor

Because no photometer perfectly aligns with the V (λ) curve, it becomes necessary to assess the proximity to this curve. A photometer's output condenses the spectral range into a single numerical value through internal integration. However, discrepancies arise when photometers assess light sources with spectral distributions diverging from the CIE Illuminant A, leading to spectral mismatch errors. Correcting this discrepancy involves employing a spectral mismatch correction factor [1, 8]

When a photometer measures a light source with a spectral power distribution differing from the calibrated standard source, it introduces an error. Rectifying this spectral mismatch error demands characterizing the photometer's relative spectral responsivity. The spectral mismatch correction factor, denoted as SCF, is derived through this characterization [9, 10].

$$SCF = \frac{\int_{360}^{830nm} P_e^T(\lambda) \times V(\lambda)\, d\lambda \int_{all-wavelengths} P_e^S(\lambda) \times R(\lambda)\, d\lambda}{\int_{all-wavelengths} P_e^T(\lambda) \times R(\lambda)\, d\lambda \int_{360}^{830nm} P_e^S(\lambda) \times V(\lambda)\, d\lambda} \qquad (1)$$

where

$P_e^T(\lambda)$: is the relative spectral output of the test source.

$P_e^S(\lambda)$: is the relative spectral output of the standard source.

$R(\lambda)$: is the relative spectral responsivity of the photometer.

$V(\lambda)$: is the spectral luminous efficiency function, which defines a photometric measurement.

2.2 Determination of Chromaticity Color Coordinates

Understanding the chromaticity color coordinates aids in evaluating the suitability of each lamp type for specific lighting applications where color accuracy, fidelity, and aesthetic considerations are crucial. These coordinates serve as vital tools for designers, manufacturers, and researchers, assisting in the selection of appropriate lighting solutions and ensuring consistent and desirable color appearances across diverse settings and environments, such as architectural lighting, outdoor illumination, or artistic displays. If spectral of irradiance E (λ) are made at the corresponding wavelengths, the tristimulus response are [6]:

$$X = \sum_i E_i \bar{x}_i, \qquad Y = \sum_i E_i \bar{y}_i \text{ , and } \qquad Z = \sum_i E_i \bar{z}_i \qquad (2)$$

Where $\bar{x}_i$, $\bar{y}_i$ and $\bar{z}_i$ are tabulated values of the tristimulus response functions.

E_i is the (relative) spectral irradiance at wavelength i

$$x = \frac{\sum E_i \bar{x}_i}{\sum E_i \bar{t}_i} \quad , \quad y = \frac{\sum E_i \bar{y}_i}{\sum E_i \bar{t}_i} \text{ and } \quad \bar{t}_i = \bar{x}_i + \bar{y}_i + \bar{z}_i \qquad (3)$$

The (u, v) transforms of (x, y) can be rewritten as

$$u = \frac{4X}{(X + 15Y + 3Z)} \quad \text{and} \quad v = \frac{6Y}{(X + 15Y + 3Z)}$$

In 1979 UCS ($\bar{u}$, $\bar{v}$) chromaticity color coordinates are a simple rescaling of the superseded (u, v) as $\bar{u} = u$ and $\bar{v} = 3v/2$

The (u, v) transforms of (x, y) can be rewritten as

$$\bar{u} = \frac{4X}{(X + 15Y + 3Z)} \quad \text{and} \quad \bar{v} = \frac{18Y}{2(X + 15Y + 3Z)} \qquad (4)$$

2.3. The Uncertainty Equations

The Guide to the Expression of Uncertainty in Measurement (GUM) gives the Law of Propagation of Uncertainty.

$$u_c^2(y) = \sum_{i=1}^{n} \left(\frac{\partial f}{\partial x_i} \right)^2 u^2(x_i) + 2 \sum_{i=1}^{n-1} \sum_{j=i+1}^{n} \frac{\partial f}{\partial x_i} \frac{\partial f}{x_j} u(x_i, x_j) \qquad (5)$$

which applies for a measurement model of the following form.

$$Y = f(X_1, X_2, X_3 ....., X_i, ...) \qquad (6)$$

where an estimate x_i of quantity X_i *has* an associated uncertainty $u(x_i)$, the squared combined standard uncertainty (the combined variance) is the sum of two terms in equation (6). The first term is the sum of the squares of the standard uncertainties $u(x_i)$ (the sum of the variances) associated with each individual effect multiplied by the relevant sensitivity coefficient (the partial derivative) [5,11]. By applying the law of propagation of uncertainty [12,13] as the following equation:

$$u^2 = \sum_{\text{var}iable} \left(\frac{\partial f_1^{'}}{\partial \text{var}iable} \right)^2 \times u^2(\text{var}iale) \qquad (7)$$

2.3.1 The Uncertainty Equations of Spectral Mismatch Factor

Hence, we have

$$u^2(SCF) = \delta^2 P_{iS} \left(\frac{\partial SCF}{\partial P_{iS}} \right)^2 + \delta^2 P_{it} \left(\frac{\partial SCF}{\partial P_{it}} \right)^2 + \delta^2 R_i \left(\frac{\partial SCF}{\partial R_i} \right)^2 \qquad (8)$$

then

P_{iS} **:** the summation of $P_e^S(\lambda)$ within the visible wavelengths range.

P_{it} **:** the summation of $P_e^T(\lambda)$ within the visible wavelengths range.

R_i **:** the summation of $R(\lambda)$ within the visible wavelengths range.

Then from equation (5) we have [14]

$$u(SCF) = \sqrt{\delta^2 P_{iS} \left(\frac{\partial SCF}{\partial P_{iS}} \right)^2 + \delta^2 P_{it} \left(\frac{\partial SCF}{\partial P_{it}} \right)^2 + \delta^2 R_i \left(\frac{\partial SCF}{\partial R_i} \right)^2} \qquad (9)$$

2.3.2 The Uncertainty Equations of Chromaticity Color Coordinates

From the propagation law of uncertainty [5], the square of the standard uncertainty in x and y is given by [7, 15-19]

$$u_c^2(x) = \sum\left(\frac{\partial x}{\partial E_i}\right)u^2(E_i) \tag{10}$$

$$u_c(x) = \frac{\sqrt{\sum E_i^2 \bar{x}_i^2 - 2x\sum E_i^2 \bar{x}_i \bar{t}_i + x^2 E_i^2 \bar{t}_i^2}}{\sum E_i \bar{t}_i} \tag{11}$$

and

$$u_c^2(y) = \sum_i\left(\frac{\partial y}{\partial E_i}\right)u^2(E_i) \tag{12}$$

$$u_c(y) = \frac{\sqrt{\sum E_i^2 \bar{y}_i^2 - 2y\sum E_i^2 \bar{y}_i \bar{t}_i + y^2 E_i^2 \bar{t}_i^2}}{\sum E_i \bar{t}_i} \tag{13}$$

From the propagation law of uncertainty [5], the square of the standard uncertainty in *u* and *v* is given by [7, 7, 15-19]

$$u_c(u) = \frac{\sqrt{\left[(u-4)^2\sum E_i^2 \bar{x}_i^2 + u^2(225\sum E_i^2 \bar{y}_i^2 + 9\sum E_i^2 \bar{z}_i^2) + 30u(u-4)\sum E_i^2 \bar{x}_i \bar{y}_i + 6u(u-4)\sum E_i^2 \bar{x}_i \bar{z}_i + 90u^2\sum E_i^2 \bar{y}_i \bar{z}_i)\right]}}{\sum E_i \bar{x}_i + \sum 15E_i \bar{y}_i + 3\sum E_i \bar{z}_i} \tag{14}$$

And

$$u_c(v) = \frac{\sqrt{\left[9(5v-2)^2\sum E_i^2 \bar{y}_i^2 + v^2(\sum E_i^2 \bar{x}_i^2 + 9\sum E_i^2 \bar{z}_i^2) + 6v(5v-2)\sum E_i^2 \bar{x}_i \bar{y}_i + 6v^2\sum E_i^2 \bar{x}_i \bar{z}_i + 18v(5v-2)\sum E_i^2 \bar{y}_i \bar{z}_i)\right]}}{\sum E_i \bar{x}_i + \sum 15E_i \bar{y}_i + 3\sum E_i \bar{z}_i} \tag{15}$$

From the propagation law of uncertainty [5], the square of the standard uncertainty in *u* and *v* is given by [7, 15-19]

$$u_c(\bar{u}) = \frac{\sqrt{\left[(\bar{u}-4)^2\sum E_i^2 \bar{x}_i^2 + \bar{u}^2(225\sum E_i^2 \bar{y}_i^2 + 9\sum E_i^2 \bar{z}_i^2) + 30\bar{u}(\bar{u}-4)\sum E_i^2 \bar{x}_i \bar{y}_i + 6\bar{u}(\bar{u}-4)\sum E_i^2 \bar{x}_i \bar{z}_i + 90\bar{u}^2\sum E_i^2 \bar{y}_i \bar{z}_i)\right]}}{\sum E_i \bar{x}_i + \sum 15E_i \bar{y}_i + 3\sum E_i \bar{z}_i} \tag{16}$$

And

$$u_c(\bar{v}) = \frac{\sqrt{\left[9(5\bar{v}-2)^2\sum E_i^2 \bar{y}_i^2 + \bar{v}^2(\sum E_i^2 \bar{x}_i^2 + 9\sum E_i^2 \bar{z}_i^2) + 6\bar{v}(5\bar{v}-2)\sum E_i^2 \bar{x}_i \bar{y}_i + 6\bar{v}^2\sum E_i^2 \bar{x}_i \bar{z}_i + 18\bar{v}(5\bar{v}-2)\sum E_i^2 \bar{y}_i \bar{z}_i)\right]}}{\sum E_i \bar{x}_i + \sum 15E_i \bar{y}_i + 3\sum E_i \bar{z}_i} \tag{17}$$

III. Experiments and Measurements

A spectroradiometer was employed to gauge the lamps' relative spectral output. The arrangement for assessing the spectral power distribution of the lamps, as depicted in Figure 2 involved direct measurement using the photometric bench and the Spectroradiometer ocean optics HR 2000 at NIS, yielding results with an uncertainty of 4.7% [20, 21]. The spectral power distribution of light was directly assessed using a photometric bench and spectroradiometer. The light under examination was directed into the spectroradiometer via an optical fiber, and its spectrum was transmitted to a computer through a USB port for data collection. Utilizing an optical fiber for light input allowed for adaptable measurement setups. The measurement method followed the CIE 63-1984 recommended by the International Electrotechnical Commission (IEC) [22]. Periodic calibration of the spectroradiometer was done using ASTM G138 standards method [23]. Spectroradiometers are highly accurate in assessing the spectral energy distribution of various light sources. Lamps being studied were individually

positioned half a meter above the spectroradiometer, and after a five-minute interval, data for each lamp was recorded. All measurements took place in a controlled dark environment with regulated temperature $(25 \pm 2)^0 C$. The electrical control parameters utilized for measuring the NIS OSRAM total luminous flux secondary and working standard lamps. The working standard lamps categorized into six groups based on wattage 25 Watts, 40 Watts, 60 Watts, 75 Watts, 100 Watts, and 200 Watts—were calibrated while positioned vertically with caps up. The precision of lamp current was estimated to be better than ±0.03% for 25W lamps and ±0.07% for other types. These lamps, initially aged and selected by OSRAM Lamp Company, underwent no further aging in the NIS laboratory. Post recalibration using the NIS OSRAM total luminous flux secondary standard lamp (calibrated at NPL in England) with an uncertainty of 0.8%, the measurements were obtained [20, 24, and 25]. In this study, seven distinct outdoor lamps were examined: Neon, Mercury, Mercury Vapor, Low Pressure Sodium, Ceramic Metal Halide, High Pressure Sodium, and Metal Halide Lamps [26,27].

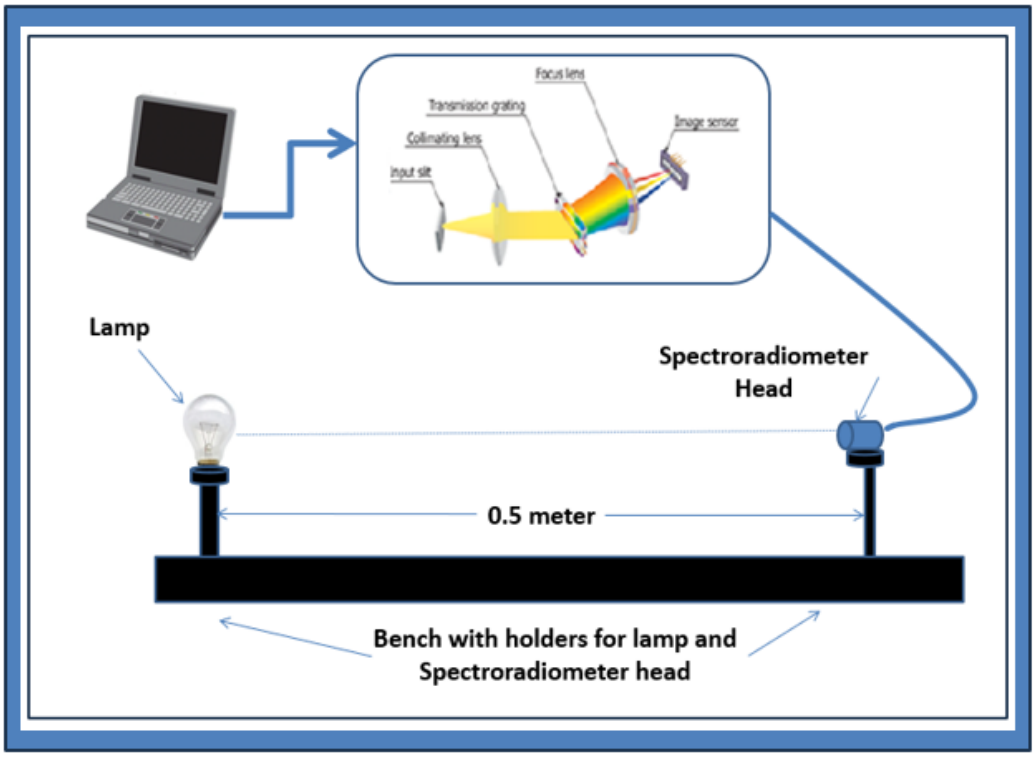

Figure 2. NIS setup for measuring the spectral power distribution.

IV. Results and Discussions

Figure 3. Illustrates spectral power distribution (SPD) diagrams for seven distinct outdoor lamps and the NIS secondary standards lamp across the visible spectrum (400 to 700 nanometers). These diagrams depict how each lamp emits radiant power within the range perceived by the human eye. Comparing these SPD diagrams against the human response curve V(λ) reveals how each lamp's emitted light aligns with human visual perception. This comparison offers insights into the interaction between the radiant power emitted by each lamp and human visual sensitivity, aiding in understanding their spectral characteristics. Each lamp type showcases unique spectral distributions through varying peaks and patterns across the visible spectrum in the SPD diagrams. These distinctive peaks or patterns highlight the specific wavelengths at which each lamp emits light most prominently. Overall, Figure 3 visually compares how these outdoor lamps emit radiant power across the visible spectrum, allowing for a comprehensive analysis of their spectral characteristics and their relation to human visual sensitivity. Understanding these spectral power distributions assists in evaluating the lamps' suitability for diverse outdoor lighting applications, encompassing considerations like color rendering, energy efficiency, and visibility.

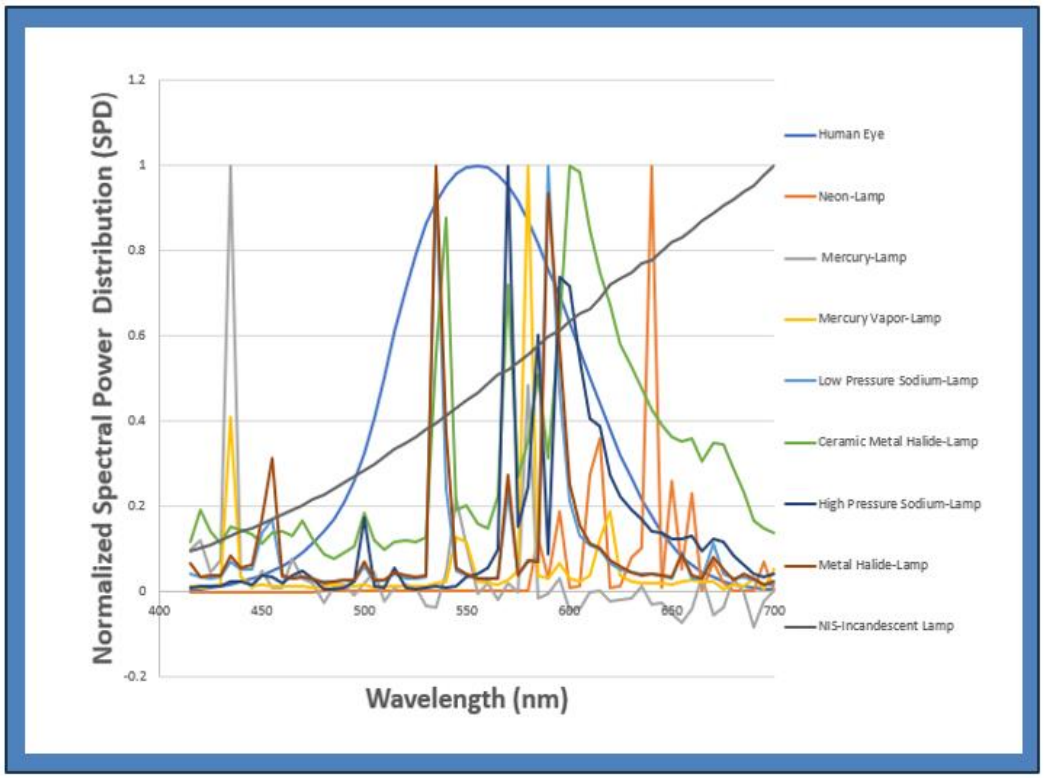

Figure 3. Spectral power distribution (SPD) diagrams across the visible spectrum for seven different types of outdoor lamps

The spectral mismatch factor played a critical role in evaluating how closely the spectral distribution of seven distinct outdoor lamps aligns with the ideal spectral output represented by the NIS standard lamps. The lamps examined included Neon, Mercury, Mercury Vapor, Low Pressure Sodium, Ceramic Metal Halide, High Pressure Sodium, and Metal Halide Lamps. Figure (4) displays the results of these mismatch factors, representing the degree of similarity or deviation between each lamp's spectral output and the ideal standard. A factor near 1 indicates a closer match, while deviations from 1 signify larger differences between the lamp's output and the standard, offering insights into how effectively each lamp replicates desired spectral qualities for outdoor lighting applications, such as color rendering and energy efficiency. This comprehensive analysis contributes to improving efficiency, safety, and quality in outdoor lighting systems, benefiting various settings and applications.

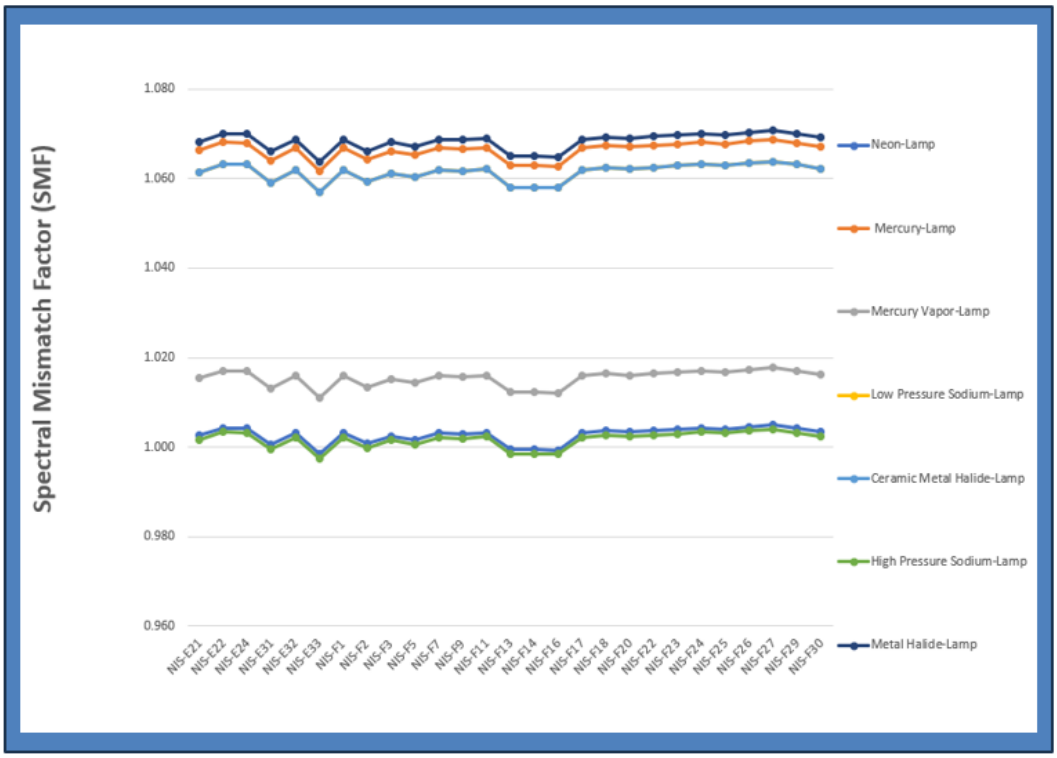

Figure 4. Spectral mismatch factor values for the outdoor lamps against NIS secondary and working standard Lamps.

In Table (1), The results of chromaticity color coordinates using the CIE 1976 (u, v) and (u', v') uniform chromaticity scale for seven distinct lamp types: Neon, Mercury, Mercury Vapor, Low Pressure Sodium, Ceramic Metal Halide, High Pressure Sodium, and Metal Halide Lamps are presented. Derived from the lamps' spectral power distributions, these coordinates uniquely represent each lamp's color appearance within the CIE 1976 color space, showcasing differences in hue and saturation independent of brightness. Table (1) likely displays numerical values of (u, v) and (u', v') chromaticity coordinates for each lamp type. These coordinates serve to map each lamp's color within the chromaticity diagram, offering insights into the specific hues and saturation levels of their emitted light. Variations among these coordinates among different lamp types indicate differences in color appearance, facilitating comparisons and evaluations concerning color rendering, color temperature, and overall light quality.

Table (1). Chromaticity Color Coordinates for the Outdoor Lamps.

Lamp	CCT (Kelvin)	u	v	$\bar{u}$	$\bar{v}$
Neon	1000	0.3693	0.3632	0.3693	0.5449
Mercury	24382	0.1976	0.3336	0.1976	0.5005
Mercury Vapor	4495	0.2617	0.3634	0.2617	0.5451
Low Pressure Sodium	1701	0.2693	0.3500	0.2693	0.5249
Ceramic Metal Halide	2378	0.2724	0.3505	0.2724	0.5257
High Pressure Sodium	1732	0.2999	0.3609	0.2999	0.5413
Metal Halide	3436	0.2546	0.3501	0.2546	0.5252

The results outlining the uncertainty tied to the spectral mismatch factor across seven distinct outdoor lamps in contrast to NIS standard lamps are extensively presented in Tables (2) to (9). These tables comprehensively capture the degree of uncertainty associated with the spectral mismatch factor, shedding light on the range of variability and possible margins of error inherent in these measurements. This data offers a nuanced understanding of the potential discrepancies and variances in these specific spectral measurements when compared to the NIS standard. Additionally, it delves into the intricacies of the spectral characteristics of outdoor lamps, providing valuable insights into their performance and deviation from the established standard.

Table (2). The Uncertainty of the Spectral Mismatch Factor for the outdoor lamps against NIS Secondary Standard Lamps (CT=2750 Kelvin)

Lamp	NIS-E21	NIS-E22	NIS-E24
Neon	0.01525	0.01526	0.01526
Mercury	0.03367	0.03367	0.03367
Mercury Vapor	0.02379	0.02379	0.02379
Low Pressure Sodium	0.01501	0.01502	0.01501
Ceramic Metal Halide	0.00543	0.00545	0.00545
High Pressure Sodium	0.01072	0.01074	0.01073
Metal Halide	0.01416	0.01417	0.01416

Table (3). The Uncertainty of the Spectral Mismatch Factor for the outdoor lamps against NIS Secondary Standard Lamps (CT=2400 Kelvin)

Lamp	NIS-E31	NIS-E32	NIS-E33
Neon	0.01509	0.01506	0.01503
Mercury	0.03384	0.03403	0.03393
Mercury Vapor	0.02387	0.02412	0.02401
Low Pressure Sodium	0.01524	0.01530	0.01535
Ceramic Metal Halide	0.00563	0.00602	0.00599
High Pressure Sodium	0.01072	0.01112	0.01106
Metal Halide	0.01441	0.01446	0.01452

Table (4). The Uncertainty of the Spectral Mismatch Factor for the outdoor lamps against NIS working Standard Lamps (CT=2351Kelvin)

Lamp	NIS-F1	NIS-F2	NIS-F3	NIS-F4	NIS-F5
Neon	0.01512	0.01533	0.01512	0.01498	0.01508
Mercury	0.03395	0.03401	0.03406	0.03459	0.03403
Mercury Vapor	0.02407	0.02411	0.02417	0.02469	0.02413
Low Pressure Sodium	0.01519	0.01562	0.01541	0.01614	0.01535
Ceramic Metal Halide	0.00610	0.00630	0.00606	0.00741	0.00594
High Pressure Sodium	0.01116	0.01140	0.01112	0.01197	0.01104
Metal Halide	0.01437	0.01479	0.01457	0.01538	0.01452

Table (5). The Uncertainty of the Spectral Mismatch Factor for the outdoor lamps against NIS working Standard Lamps (CT=2693Kelvin)

Lamp	NIS-F7	NIS-F9
Neon	0.01516	0.01518
Mercury	0.03378	0.03374
Mercury Vapor	0.02387	0.02384
Low Pressure Sodium	0.01511	0.01506
Ceramic Metal Halide	0.00553	0.00551
High Pressure Sodium	0.01080	0.01080
Metal Halide	0.01427	0.01422

Table (6). The Uncertainty of the Spectral Mismatch Factor for the outdoor lamps against NIS working Standard Lamps (CT=2761Kelvin)

Lamp	NIS-F11	NIS-F13	NIS-F14
Neon	0.01519	0.01515	0.01519
Mercury	0.03375	0.03379	0.03369
Mercury Vapor	0.02386	0.02390	0.02381
Low Pressure Sodium	0.01504	0.01505	0.01501
Ceramic Metal Halide	0.00553	0.00547	0.00542
High Pressure Sodium	0.01080	0.01076	0.01072
Metal Halide	0.01420	0.01420	0.01416

Table (7). The Uncertainty of the Spectral Mismatch Factor for the outdoor lamps against NIS working Standard Lamps (CT= 2737Kelvin)

Lamp	NIS-F16	NIS-F17	NIS-F18	NIS-F20
Neon	0.01517	0.01516	0.01521	0.01521
Mercury	0.03375	0.03378	0.03371	0.03370
Mercury Vapor	0.02387	0.02387	0.02384	0.02383
Low Pressure Sodium	0.01507	0.01511	0.01506	0.01505
Ceramic Metal Halide	0.00549	0.00553	0.00546	0.00549
High Pressure Sodium	0.01077	0.01080	0.01076	0.01077
Metal Halide	0.01423	0.01427	0.01421	0.01421

Table (8). The Uncertainty of the Spectral Mismatch Factor for the outdoor lamps against NIS working Standard Lamps (CT=2788Kelvin)

Lamp	NIS-F22	NIS-F23	NIS-F24	NIS-F25
Neon	0.01525	0.01523	0.01525	0.01525
Mercury	0.03368	0.03368	0.03368	0.03369
Mercury Vapor	0.02380	0.02380	0.02381	0.02381
Low Pressure Sodium	0.01499	0.01503	0.01503	0.01501
Ceramic Metal Halide	0.00545	0.00545	0.00545	0.00547
High Pressure Sodium	0.01072	0.01076	0.01074	0.01077
Metal Halide	0.01414	0.01418	0.01418	0.01416

Table (9). The Uncertainty of the Spectral Mismatch Factor for the outdoor lamps against NIS working Standard Lamps (CT=2790Kelvin)

Lamp	NIS-F26	NIS-F27	NIS-F29	NIS-F30
Neon	0.01526	0.01523	0.01526	0.01527
Mercury	0.03369	0.03375	0.03366	0.03366
Mercury Vapor	0.02383	0.02388	0.02378	0.02379
Low Pressure Sodium	0.01502	0.01500	0.01500	0.01500
Ceramic Metal Halide	0.00545	0.00550	0.00546	0.00544
High Pressure Sodium	0.01076	0.01082	0.01073	0.01072
Metal Halide	0.01417	0.01420	0.01415	0.01416

The results outlining the uncertainty tied to chromaticity color coordinates across seven distinct outdoor lamps are extensively presented in Tables (10).

Table (10). The Uncertainty of Chromaticity Color Coordinates for the outdoor lamps.

Lamp	$u_c(u)$	$u_c(v)$	$u_c(\bar{u})$	$u_c(\bar{v})$
Neon	4.72	1.44	4.72	1.26
Mercury	0.83	4.04	0.83	3.56
Mercury Vapor	1.53	2.23	1.53	1.97
Low Pressure Sodium	1.24	1.44	1.24	1.27
Ceramic Metal Halide	1.14	0.56	1.14	0.49
High Pressure Sodium	1.44	1.18	1.44	1.04
Metal Halide	0.85	1.32	0.85	1.16

V. Conclusions

Outdoor lighting holds a vital role in ensuring nighttime safety and security by brightening public areas to prevent crime and assist with navigation. Additionally, it prolongs the time for outdoor activities, promoting community gatherings and leisure. Moreover, these lights improve the visual appeal of outdoor spaces, highlighting architectural elements and landscapes, contributing to the overall atmosphere of the environment. The spectral power distribution (SPD) diagrams depict distinctive lamp responses characterized by narrow peaks in their spectral distribution. Each lamp exhibits unique characteristics, emitting their spectrum in the visible region with varying distributions. Figure (4) displays the disparity factors between the spectral output of various lamps and the ideal standard. Factors nearing 1 indicate a closer resemblance, while larger deviations signal greater differences. This figure details the spectral mismatch correction factor for seven outdoor lamp types: Neon, Mercury, Mercury Vapor, Low Pressure Sodium, Ceramic Metal Halide, High Pressure Sodium, and Metal Halide Lamps. It reveals that these lamp types' spectral power distributions don't perfectly align with the human response curve V (λ) and the photometer response. The High Pressure Sodium lamp demonstrates the lowest value, while the Metal Halide lamp shows the highest. Meanwhile, Table (1) outlines the chromaticity color coordinates for these lamps, while Tables (2) through (10) provide uncertainty estimations for both the spectral mismatch correction factor and the Chromaticity Color Coordinates of the seven distinct outdoor lamps.

References

[1]. Ohno, Y., Photometry Calibration, NIST Special Publication 250-37, 1996.
[2]. https://www.newport.com/t/integrating-sphere-fundamentals-and-applications.
[3]. https://www.labsphere.com/wp-content/uploads/2021/09/Integrating-Sphere-Theory-and-Applications.pdf.
[4]. Hunt, R. W. G. (2013). The Reproduction of Colour (6th ed., Vol. 1). Wiley, Fairchild, M. D. (2013). Color Appearance Models. Wiley.
[5]. Guide to the Expression of Uncertainty in Measurement, 1993, First Edition, International Organization for Standardization (ISO).
[6]. Commission International de l'Eclairage, "Colorimetry", Second Ed. CIE 15.2-1986., J. L. Gardner, „Uncertainty Estimation in Colour Measurement", Metrologia, VOL. 25, 2000.
[7]. J. L. Gardner, "Correlated colour temperature- uncertainty and estimation", Metrologia, VOL. 37, 2000.
[8]. C. Decusatis. 1998. Handbook of applied photometry. Woodbury, N.Y.: AIP Press.

[9]. A.A. Gaertner, "LED Measurement Issues", Photometry, Radiometry and Colorimetry Course NRC, Ottawa, Canada, 2007.
[10]. Manal A. Haridy, and Affia Aslam (August 1st, 2018). Optical Radiation Metrology and Uncertainty, Metrology Anil, IntechOpen, DOI: 10.5772/intechopen.75205. Available from: https://www.intechopen.com/books/metrology/optical-radiation-metrology-and-uncertainty.
[11]. International Organization for Standardization (ISO), Guide to the expression of uncertainty in measurement (1995).
[12]. Emma R. Woolliams, "Determining the uncertainty associated with integrals of spectral quantities", Metrology for solid state lighting, EMRP-ENG05-1.3.1, Version 1.0, 2013.
[13]. U. Krüger and G. Sauter. Comparison of methods for indicating the measurement uncertainty of integral parameters on the basis of spectral data by means of the measurement uncertainty of the f1' value. Proceedings of the 2nd CIE Expert Symposium on Measurement Uncertainty, CIE x029:2006, p.159-163.
[14]. Manal A. Haridy, "Uncertainty of Spectral Mismatch Factor for Spot White (LEDs) and Compact Fluorescent Lamps ", ARPN Journal of Engineering and Applied Science, VOL. 14, NO. 5, MARCH, 2019.
[15]. J. L. Gardner, "Uncertainty Estimation in Colour Measurement", Metrologia, VOL. 25, 2000.
[16]. Colorimetry, 3rd ed., International Commission on Illumination, Vienna, CIE Publication 15 (2004).
[17]. Manal A. Haridy "Color Coordinates and Uncertainty for Luminous Flux Secondary and Working Standard Lamps" American Journal of Engineering Research (AJER), vol.8, no.05, 2019, pp.273-280.
[18]. Manal A. Haridy, Manal G. Eldin, "Uncertainty Equations of Spectral Quality Factors for Photometers and Colorimeters by Using GUM Method ", ARPN Journal of Engineering and Applied Science, VOL. 13, NO. 10, MAY 2018.
[19]. Manal A. Haridy "Color Coordinates and Uncertainty for Luminous Flux Secondary and Working Standard Lamps" American Journal of Engineering Research (AJER), vol.8, no.05, pp.273-280, 2019.
[20]. Manal A. Haridy, "Improvement uncertainty of total luminous flux measurements by determining some correction factors". Int. J. Curr. Res. Aca. Rev., 3(6): 264 274, 2015.
[21]. Manal A. Haridy, "Uncertainty Estimation of Spectral Mismatch Correction Factor for Incandescent Lamps", Int. J. Curr. Res. Aca. Rev; 3(7), pp. 262-273,2015.
[22]. International Electrotechnical Commission (IEC). Spectroradiometric measurement of light sources. Vienna: CIE Publication;1984.
[23]. ASTM G138. Standard test method for calibration of a spectroradiometer using a standard source of irradiance. Pennsylvania: West Conshohocken; 2012.
[24]. Kertil, J. "Report on photometric measurements and instruction notes for calibration of photometric standards", NIS, Cairo., 1969.
[25]. Manal A. Haridy, "Uncertainty estimation of spectral mismatch correction factor for incandescent lamps". Int. J. Curr. Res. Aca. Rev., 3(7): 262 273, 2015.
[26]. LSPDD. http://galileo.graphycs.cegepsherbrooke.qc.ca/app/en/lamps, 2017.
[27]. Carlos Eugenio Tapia Ayuga, Jaime Zamorano, "LICA AstroCalc, a software from the spectra of street and indoor lamps", Journal of Quantitative spectroscopy & Radiative Transfer, Vol. 214, Pages 33-38, July 2018.